

High S100A9⁺ cell density predicts a poor prognosis in hepatocellular carcinoma patients after curative resection

Jing Liao^{1,2,3,*}, Jin-Zhu Li^{1,*}, Jing Xu⁴, Yongquan Xu¹, Wei-Ping Wen², Limin Zheng¹, Lian Li¹

¹MOE Key Laboratory of Gene Function and Regulation, School of Life Sciences, Sun Yat-sen University, Guangzhou, Guangdong 510275, China

²Division of Head and Neck Surgery, Department of Otorhinolaryngology, The Sixth Affiliated Hospital, Sun Yat-sen University, Guangzhou, Guangdong 510655, China

³Guangdong Institute of Gastroenterology, The Sixth Affiliated Hospital, Sun Yat-sen University, Guangzhou, Guangdong 510655, China

⁴State Key Laboratory of Oncology in South China, Collaborative Innovation Center for Cancer Medicine, Sun Yat-sen University Cancer Center, Guangzhou, Guangdong 510060, China

*Equal contribution

Correspondence to: Lian Li; **email:** lilian2@mail.sysu.edu.cn

Keywords: hepatocellular carcinoma, S100A9, myeloid cells, prognosis, curative resection

Received: February 26, 2021

Accepted: May 19, 2021

Published: June 22, 2021

Copyright: © 2021 Liao et al. This is an open access article distributed under the terms of the [Creative Commons Attribution License](https://creativecommons.org/licenses/by/3.0/) (CC BY 3.0), which permits unrestricted use, distribution, and reproduction in any medium, provided the original author and source are credited.

ABSTRACT

S100A9 is differentially expressed in various cell types and is associated with the development, progression and metastasis of various cancers. However, the expression, distribution, and clinical significance of S100A9 in hepatocellular carcinoma (HCC) remain unclear. In the present study, The Cancer Genome Atlas (TCGA) database was used to examine S100A9 gene expression in HCC; we found that S100A9 expression was associated with HCC prognosis. In addition, S100A9 protein expression was assessed by immunohistochemistry analysis of tissues from 382 HCC patients. We found that the infiltration of S100A9⁺ cells in both tumor and nontumor tissues could predict poor overall survival ($P = 0.0329$, tumor; $P = 0.0003$, nontumor) and a high recurrence risk ($P = 0.0387$, tumor; $P = 0.0015$, nontumor) in our tissue microarray analysis. Furthermore, immunofluorescence double staining revealed that the primary S100A9-expressing cells in adjacent nontumoral tissue were CD15⁺ neutrophils, and both CD68⁺ macrophages and CD15⁺ neutrophils expressed S100A9 in HCC tumor tissues. Taken together, the results suggest that high S100A9⁺ cell density predicts a poor prognosis in HCC patients, and S100A9 expression could potentially serve as an independent prognostic marker for HCC.

INTRODUCTION

Hepatocellular carcinoma (HCC) is one of the leading causes of cancer-related death worldwide [1, 2]. Currently, surgical resection, orthotopic liver transplantation, immunotherapy and radiofrequency thermal ablation are the most common treatments for HCC [3]. Despite significant advances, the incidence and mortality rates of HCC continue to rise. Hence, there is an urgent need for a reliable prognostic biomarker to

effectively stratify patients for appropriate treatment and to improve patient survival [4–6].

Accumulating evidence has highlighted the significance of inflammation, which dramatically affects the progression and prognosis of HCC patients. S100A9 is a calcium-binding protein that plays an indispensable role as a mediator in inflammatory processes [7]. Evidence has demonstrated that S100A9 is elevated in various solid tumors and that the upregulation of S100A9 positively

correlates with poor outcomes in colorectal, gastric, liver, pancreatic and prostate cancer [8–14]. Moreover, some researchers have observed that *S100A9* is a negative regulator of lymph node metastasis in gastric adenocarcinoma [15, 16]. These findings suggest that *S100A9* exerts antitumor or tumorigenic activity depending on the cancer type and could serve as a potential biomarker for prognosis prediction in cancer.

Solid tumors comprise not only cancer cells but also many other nonmalignant cell types, which produce a unique microenvironment that regulates tumor progression. *S100A9* is expressed mainly by neutrophils, monocytes, and activated macrophages [7, 8]. Recently, *S100A9* was also proposed as a novel marker of human monocytic myeloid-derived suppressor cells (MDSCs) [17]. Thus, it is important to define the cellular sources of *S100A9* in HCC and evaluate its association with clinicopathological factors. Herein, we investigated the expression, distribution and

prognostic significance of *S100A9* in 382 patients with HCC. Our data showed that most *S100A9*-expressing cells were neutrophils and macrophages (Mφs) in tumor tissues, and neutrophils in nontumoral tissues. Moreover, we found that either tumoral or nontumoral *S100A9*⁺ cell density can serve as an independent predictor of poor prognosis in patients with HCC.

RESULTS

High *S100A9* expression correlates with a poor prognosis in HCC patients in the TCGA-LIHC dataset

We used bioinformatics analysis to examine the association between *S100A9* expression and the prognosis of patients with HCC. According to the TCGA-LIHC dataset analysis, *S100A9* gene expression was significantly downregulated in tumor tissues compared to adjacent nontumor tissues (Figure 1A).

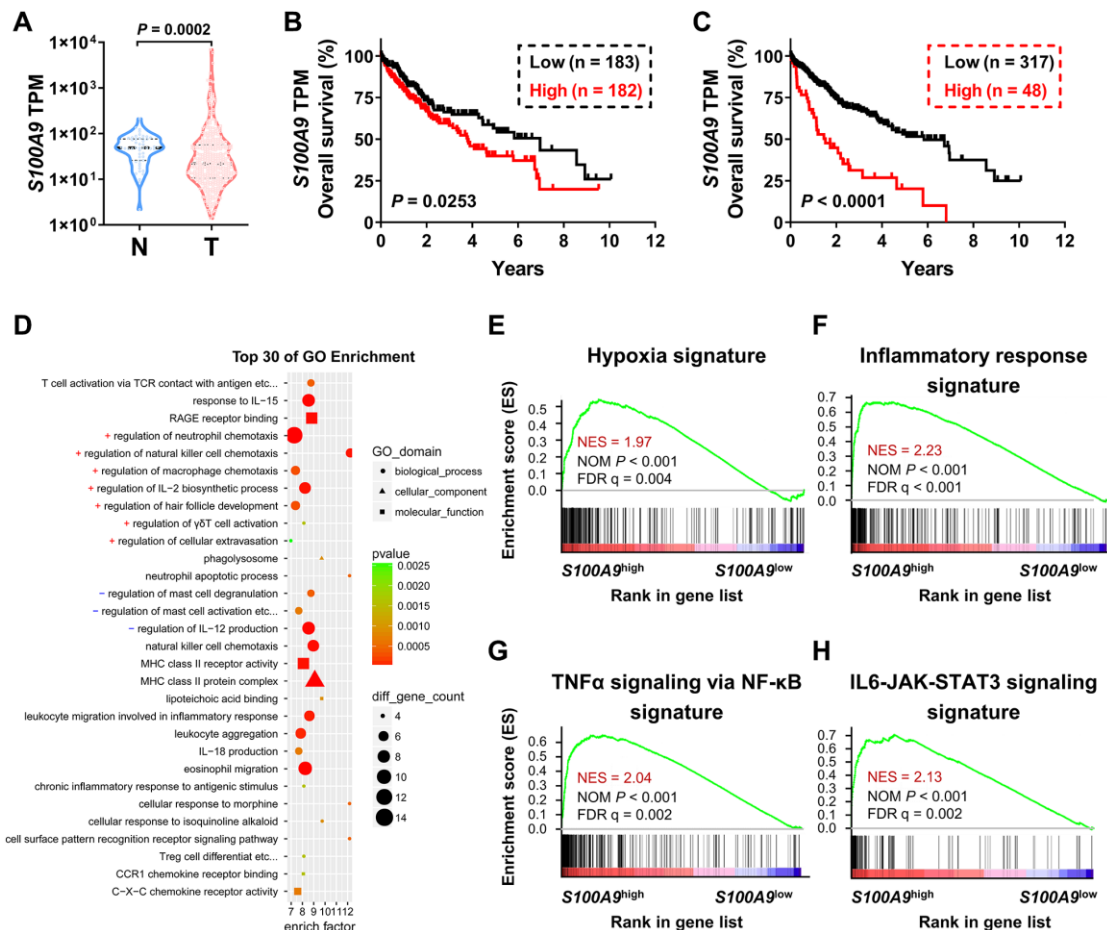


Figure 1. Association between *S100A9* expression and prognosis of HCC patients in the TCGA-LIHC database. (A) Violin plot showing the differential expression of the *S100A9* gene in tumor ($n = 365$) or nontumor ($n = 50$) tissues from the TCGA-LIHC database; the Mann-Whitney test was used to analyze the nonparametric test between the two groups. HCC patients in the TCGA dataset were divided into two groups according to the median value of *S100A9* expression (B) or minimum P -value approach (C). The prognostic value of *S100A9* was evaluated by the Kaplan-Meier method, and examined by the log-rank test. (D) Top 30 GO enrichment results of the 3493 genes highly expressed in the *S100A9*^{high} group. (E–H) Top enriched signaling pathways based on *S100A9* expression identified by GSEA.

Moreover, high S100A9 expression in tumor tissue correlated with an unfavorable prognosis in HCC patients in subgroups divided by the median value (Figure 1B) and minimum P -value approach (Figure 1C). In addition, GO and GSEA analyses were adopted to further verify the candidate genes and analyze the molecular pathways. Interestingly, *S100A9* gene expression in HCC patients was linked to “immune cell migration,” “the inflammatory response,” “hypoxia,” and “TNF- α and IL-6 signaling” (Figure 1D–1H). The above results suggested that *S100A9* gene expression was negatively associated with HCC patients’ prognosis.

S100A9 expression is associated with a poor prognosis in HCC patients

We performed IHC to assess the protein expression level of S100A9 in the HCC microarray chip. First, we applied automated measurements with computerized image analysis to count S100A9⁺ cells in HCC microarray assays (Figure 2A). To assess methodological consistency, we found that the number of S100A9⁺ cells determined by the automated enumeration method highly correlated with the number of positive cells detected by a pathologist (Figure 2B, Pearson $R = 0.9025$, $P < 0.0001$). As shown in Figure 2C, S100A9⁺ cell density was significantly higher in the nontumoral tissue than in the tumoral tissue ($P < 0.0001$).

We next investigated the prognostic role of S100A9 expression in HCC. A total of 382 treatment-naïve HCC patients who had long-term follow-up data were divided into two groups according to the median counts of S100A9⁺ cells in the tumoral region and nontumoral

region. Kaplan-Meier analysis revealed a negative association between overall survival (OS) and the density of S100A9⁺ cells in the nontumoral region ($P = 0.0003$, Figure 3A) and tumoral region ($P = 0.0329$, Figure 3C). Patients with a high density of S100A9⁺ cells in the nontumoral region or in the tumoral region had a significantly higher recurrence rate than patients with a low density of S100A9⁺ cells (nontumor, $P = 0.0015$, Figure 3B; tumor, $P = 0.0387$, Figure 3D). According to the results of the univariate analysis (Figure 3E), S100A9⁺ cell density in the nontumoral region or in the tumoral region was associated with OS. The clinicopathologic features that were significant in univariate analysis were adopted as covariates in the multivariate analysis, which revealed that S100A9⁺ cell density in the tumor region or in the nontumoral region was a powerful independent prognostic predictor for OS (Figure 3F; tumor, HR = 1.149; $P = 0.036$; nontumor, HR = 1.623; $P = 0.005$).

We also evaluated the combined influence of S100A9⁺ cells in tumor and nontumor regions. Using the median value as a cutoff, patients were classified into four groups: I, N-S100A9^{low} T-S100A9^{low} ($n = 110$); II, N-S100A9^{low} T-S100A9^{hi} ($n = 81$); III, N-S100A9^{hi} T-S100A9^{low} ($n = 81$); and IV, N-S100A9^{hi} T-S100A9^{hi} ($n = 110$). Significant differences in OS (Figure 3G) and recurrence rate (Figure 3H) were found among the four groups. Patients in group IV exhibited the worst OS (OS rate: 45.43%) among all patients, including those in group I (5-year OS rate: 66.59%; $P < 0.0001$), group II (5-year OS rate: 70.59%; $P = 0.0009$), and group III (5-year OS rate: 59.39%; $P = 0.0277$). In addition, patients in group IV exhibited the highest recurrence rate (5-year recurrence rate: 76.07%) among all patients, including those in group I (5-year recurrence rate: 53.80%; $P =$

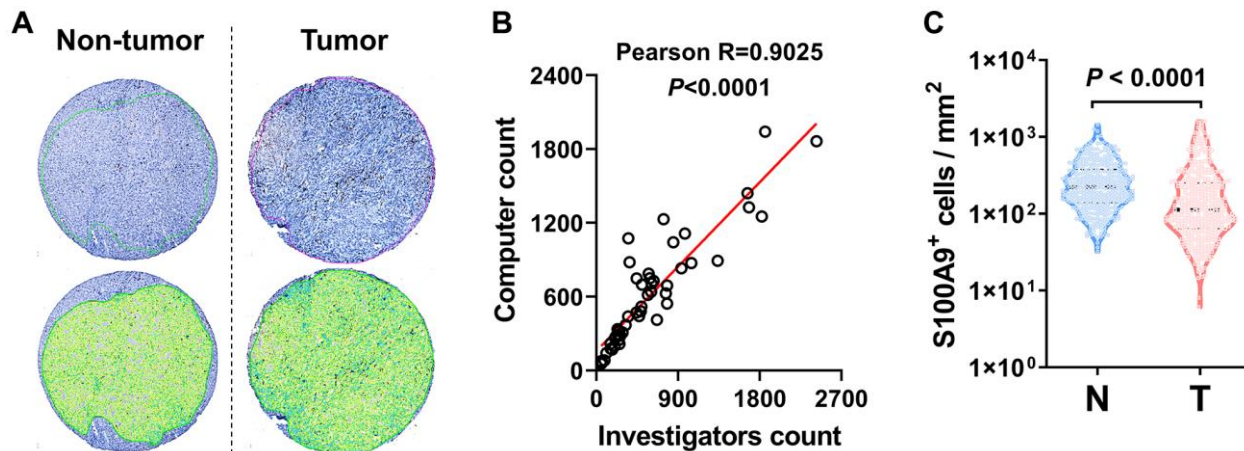


Figure 2. S100A9 expression in HCC tumor. (A) Representative images of IHC staining. (B) Scatter plot illustrating the correlation between S100A9-expressing cell counts in HCC by computer counting and investigator counting. (C) Quantification of S100A9⁺ cell densities in the N (nontumoral) and T (tumoral) regions ($n = 382$), and the Wilcoxon matched-pairs signed-rank test was used to analyze the nonparametric test between the paired two groups.

0.0004), group II (5-year recurrence rate: 55.53%; $P = 0.0137$), and group III (5-year recurrence rate: 69.34%; $P = 0.1279$). The above data suggest that S100A9 might represent a potential target for HCC therapy.

We also analyzed the correlation between S100A9⁺ cell density and patient clinicopathological features. Table 1 shows that the tumoral S100A9⁺ cell number did not significantly correlate with patient sex, age, HBsAg, AFP, ALT, cirrhosis, differentiation, tumor multiplicity, tumor size, Barcelona Clinic Liver Cancer (BCLC) stage or TNM stage. However, nontumoral S100A9⁺ cell density, but not tumoral S100A9⁺ cell density, was associated with sex, tumor size, BCLC stage and TNM stage.

S100A9 expression correlates with myeloid cell infiltration in the tumor microenvironment

To investigate the relationship between S100A9 expression and the immune system, we adopted the

CIBERSORT algorithm [18] to evaluate the association between S100A9 gene expression and tumor immune cell infiltration using the TCGA-LIHC data set. Only 7 nontumoral and 49 tumoral samples with a CIBERSORT P -value < 0.05 were retained for further study. The abundances of twenty-two immune cell types in each HCC sample are presented in the boxplot in Figure 4A. The results indicated that the infiltration of immune cells was not significantly related to the expression of the S100A9 gene (data not shown). However, in terms of the component of cells, macrophages (M0 + M1 + M2 Mφ) were the main cell populations in the microenvironment of HCC tumor tissue. Hence, we investigated the prognostic significance of Mφs in 49 patients in the TCGA-LIHC dataset. As shown in Figure 4B–4E, the M0, M1 and M2 Mφ densities did not correlate with the survival of HCC patients. However, patients with a high density of Mφs had significantly shorter OS than patients with a low Mφ density. Moreover, the association among the density of S100A9⁺ cells, CD15⁺ neutrophils and

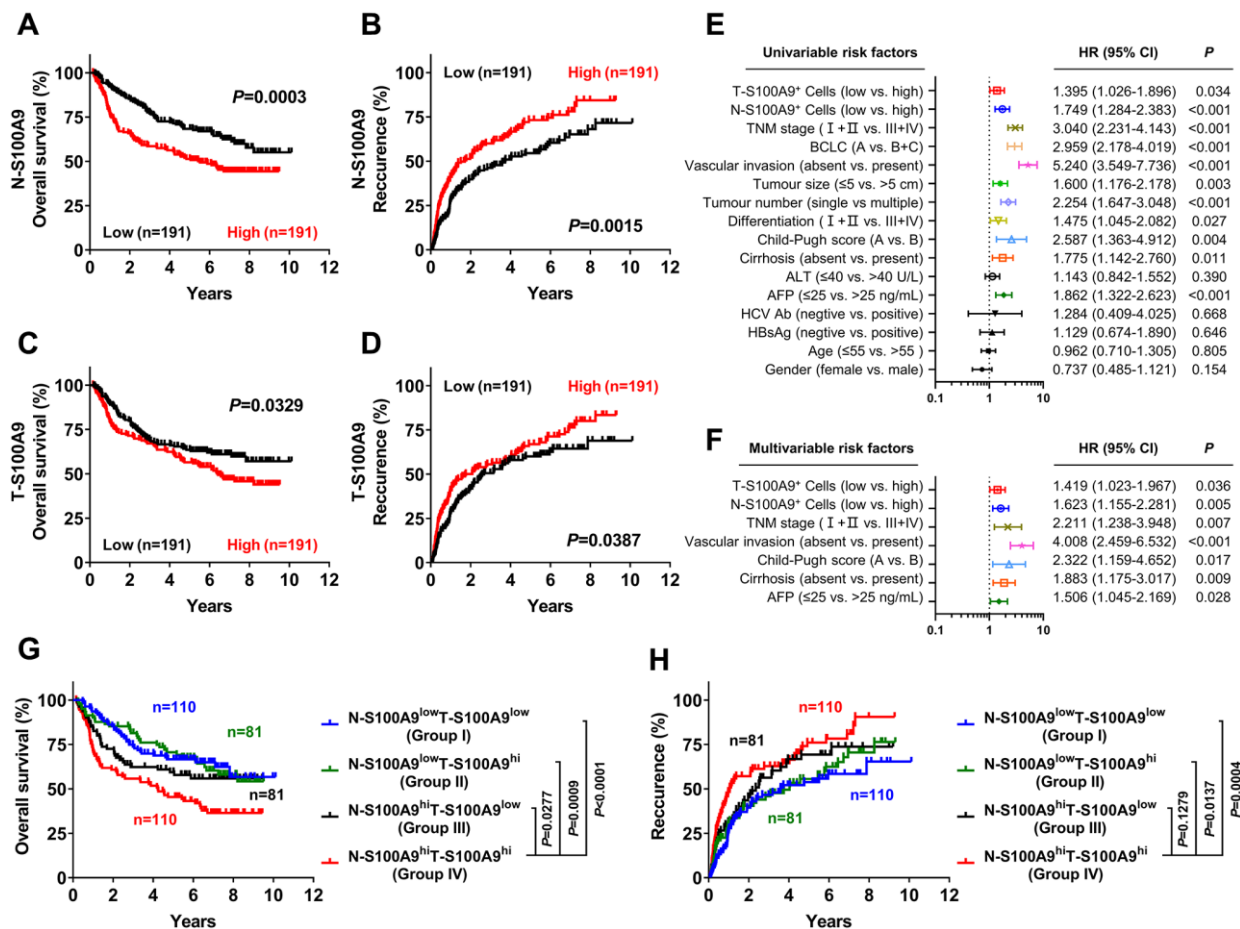


Figure 3. Prognostic value of S100A9⁺ cell in HCC patients. A high S100A9⁺ cell density in nontumor or tumor tissue was associated with poor OS (A, C) and a high recurrence rate (B, D) in HCC patients. Forest plots showing the association between S100A9 expression in tumors and clinicopathological features in HCC patients using univariate (E) or multivariate analysis (F). Patients were divided into two groups according to the median value of the S100A9⁺ cell density in nontumoral and tumoral tissues. The cumulative OS (G) and recurrence (H) times were calculated using the Kaplan-Meier method and then analyzed with the log-rank test.

CD68⁺ Mφ infiltration in our tissue microarray was analyzed (Figure 4F). The density of S100A9⁺ cells was positively associated with the infiltration of CD15⁺ cells and CD68⁺ cells in both the nontumoral and tumoral regions.

Cellular source of S100A9⁺ cells

S100A9 is expressed in a heterogeneous population of cells [7, 8]. Multicolor immunofluorescence staining was performed to characterize the cellular source of S100A9⁺ cells in HCC. S100A9 was expressed at low levels in CD34⁺ endothelial cells and CD3⁺ T cells and was not detected in CD56⁺ NK cells or CD20⁺ B cells

(Figure 5). As expected, S100A9 protein was mainly expressed in myeloid cells. We found that neutrophils predominantly infiltrated the nontumoral area rather than the tumoral area, and CD15⁺ cells were the main cell population that expressed S100A9 protein ($58.19 \pm 20.80\%$) in nontumor areas, but this proportion was significantly reduced in tumor areas ($29.01 \pm 24.20\%$) (Figure 6A–6C). In addition, $39.69 \pm 17.30\%$ of S100A9⁺ cells in the tumoral region were CD68⁺ cells, but only $12.23\% \pm 7.17\%$ of S100A9⁺ cells in the nontumoral region were CD68⁺ cells (Figure 6D–6F). Collectively, our findings indicated that the primary S100A9-expressing cells in adjacent nontumoral tissue are CD15⁺ neutrophils, and both CD68⁺ Mφs and

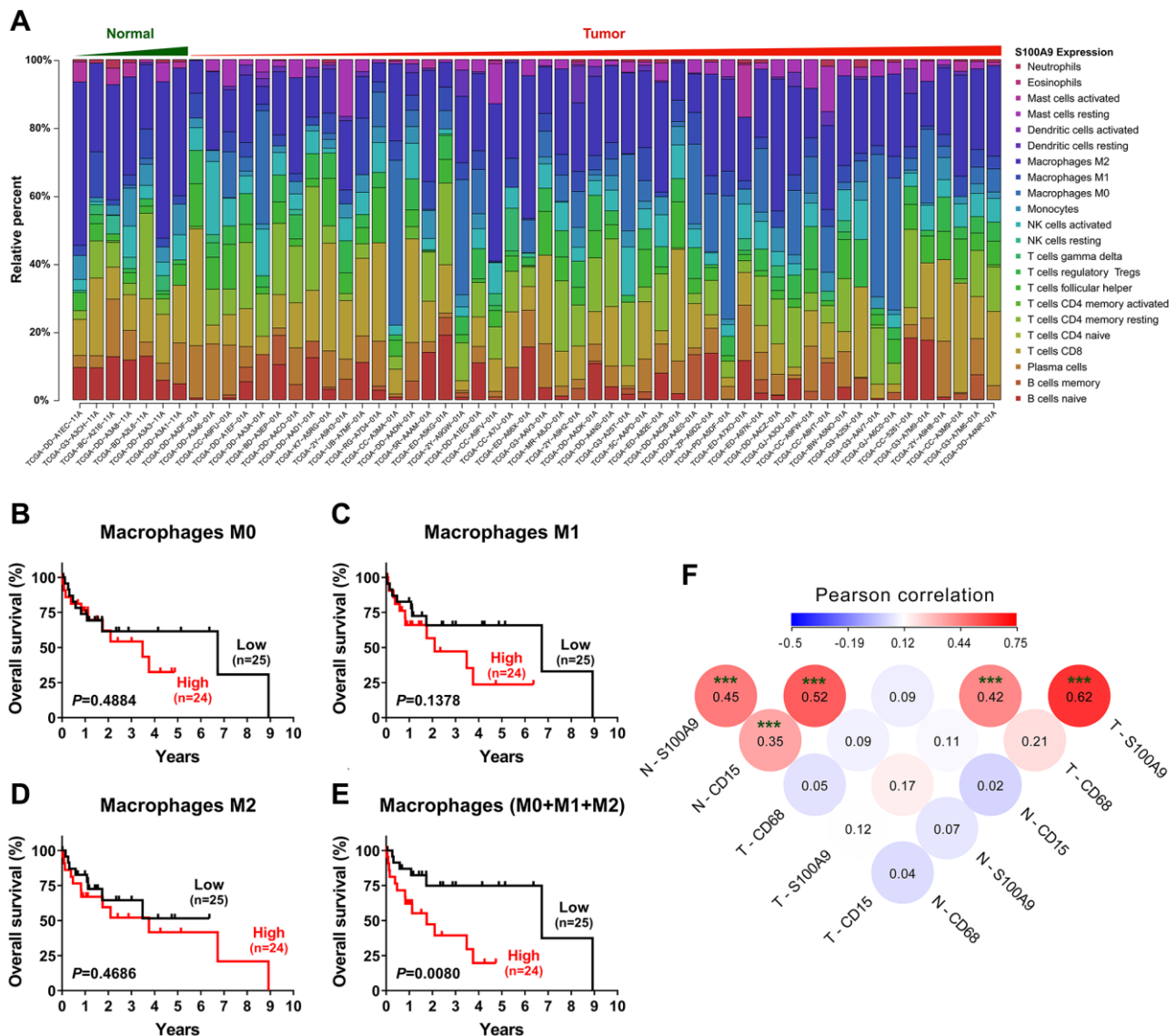


Figure 4. Tumor-infiltrating immune cells associated with S100A9 expression in HCC. (A) Differential infiltration of immune cells based on S100A9 expression in groups from the TCGA-LIHC cohort. The proportions of 22 immune infiltrates in tumor ($n = 49$) and nontumor tissue ($n = 7$) were estimated using the CIBERSORT algorithm. (B–E) Prognostic value of M0, M1, M2 and total (M0 + M1 + M2) macrophage densities in HCC ($n = 49$). (F) The densities of S100A9⁺ cells and CD15⁺ neutrophils and CD68⁺ macrophages were analyzed using Pearson correlation analysis ($n = 382$). *** $P < 0.001$.

CD15⁺ neutrophils highly express S100A9 in HCC tumor tissues.

DISCUSSION

S100 proteins are involved in a variety of biological processes and expressed in various cell types in tissues. We delineated the distribution and prognostic value of

S100A9⁺ cells in HCC tissue. A high S100A9⁺ cell density in either tumoral or nontumoral tissue was found to be a predictor of unfavorable prognosis and could serve as an independent risk factor in patients with HCC. Furthermore, we demonstrated that Mφs and neutrophils accounted for most S100A9⁺ cells in HCC tumoral tissue and that neutrophils were the dominant S100A9⁺ cells distributed in nontumoral tissue.

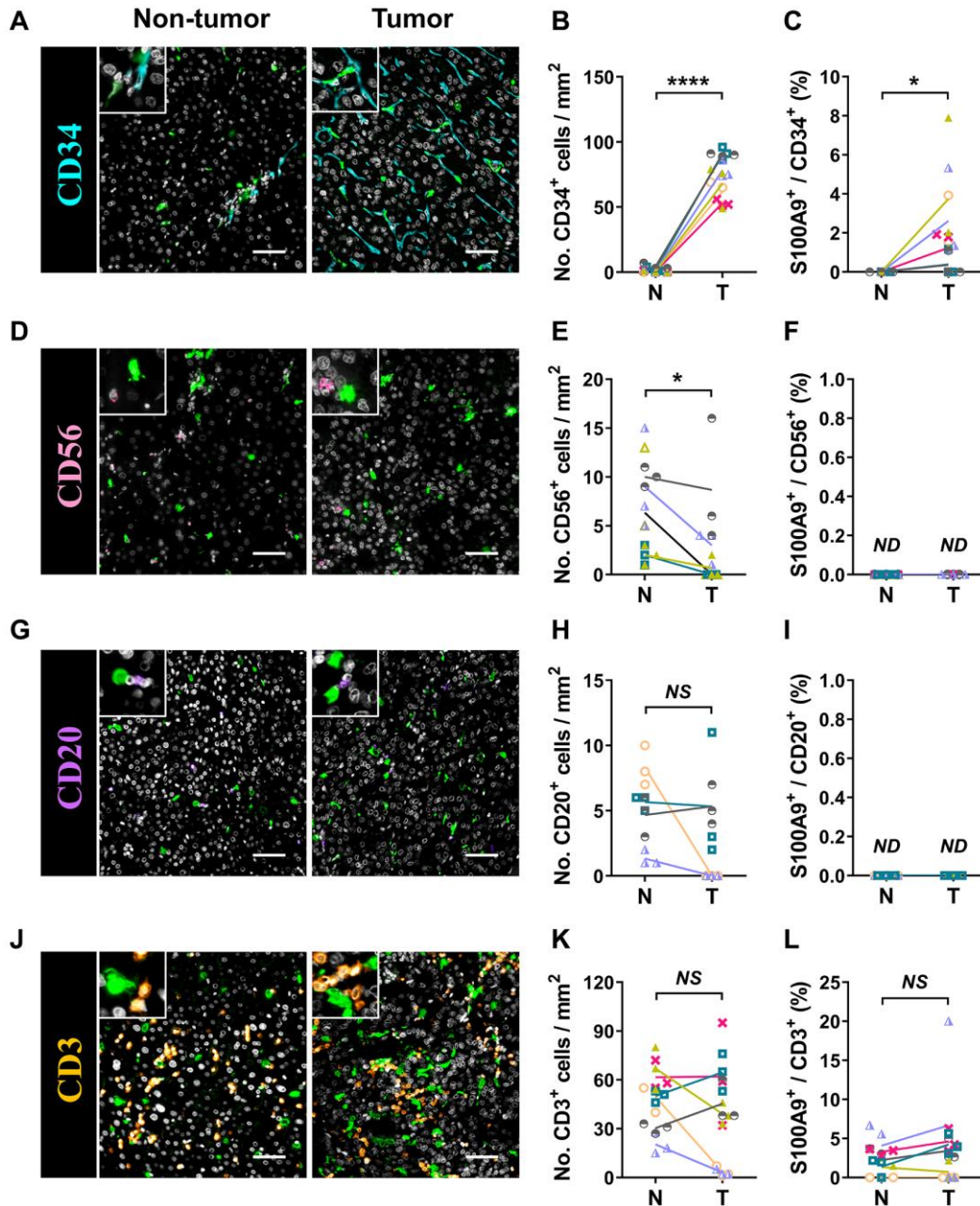


Figure 5. Characterization of patient-derived S100A9⁺ cells. Multiple immunofluorescence staining shows DAPI (gray), S100A9 (green), CD34 (blue, **A**), CD56 (pink, **D**), CD20 (purple, **G**), and CD3 (orange, **J**) expression and coexpression (double-positive cells) in HCC tissue. Quantification of CD34 (**B**), CD56 (**E**), CD20 (**H**), and CD3 (**K**) cell densities in the T and N regions. (**C**) The percentages of S100A9⁺CD34⁺ cells among the total CD34⁺ cells in the N and T regions. (**F**) The percentages of S100A9⁺CD56⁺ cells among the total CD56⁺ cells in the N and T regions. (**I**) The percentages of S100A9⁺CD20⁺ cells among the total CD20⁺ cells in the N and T regions. (**L**) The percentages of S100A9⁺CD3⁺ cells among total CD3⁺ cells in the N and T regions ($n = 4 - 7$). Scale bar = 50 μ m. The results are the means \pm SEM (bars); NS, no significance; ND, not detected.

S100A9, a member of the S100 family, is expressed in granulocytes, monocytes, macrophages, MDSCs and tumor cells in various cancers [7, 8, 17, 19, 20]. In this study, we found that S100A9 was predominately located in infiltrating Mφs and neutrophils in HCC tumoral tissue. In nontumoral tissue, neutrophils were the main source of S100A9⁺ cells. Few HCC cells themselves express S100A9. These results were consistent with those of previous studies demonstrating high S100A9 expression in infiltrating immune cells in various cancer types, including colorectal cancer and pancreatic cancer [9, 11]. In other cancer types, such as lung cancer [21], prostate cancer [22], nasopharyngeal carcinoma [23], and breast cancer [24], S100A9 is expressed mainly by neoplastic tumor cells themselves. Arai et al. found that S100A9 is expressed in malignant

hepatocytes and that high S100A9 expression is related to poorly differentiated carcinomas [25]. However, we found few S100A9-positive HCC cells, even in poorly differentiated HCC. The inconsistent results are probably due to differences in the stage, number, and size of tumors; the sample size or the antibodies used to detect S100A9 expression. Overall, high S100A9 expression on Mφs and neutrophils in HCC tissues may indicate that S100A9 plays a crucial role in HCC development.

The relationship between S100A9 expression in HCC and disease progression remains unclear. Here, we observed that high tumoral S100A9 expression at both the RNA (TCGA-LIHC data set analysis) and protein (IHC detection) levels was associated with a poor

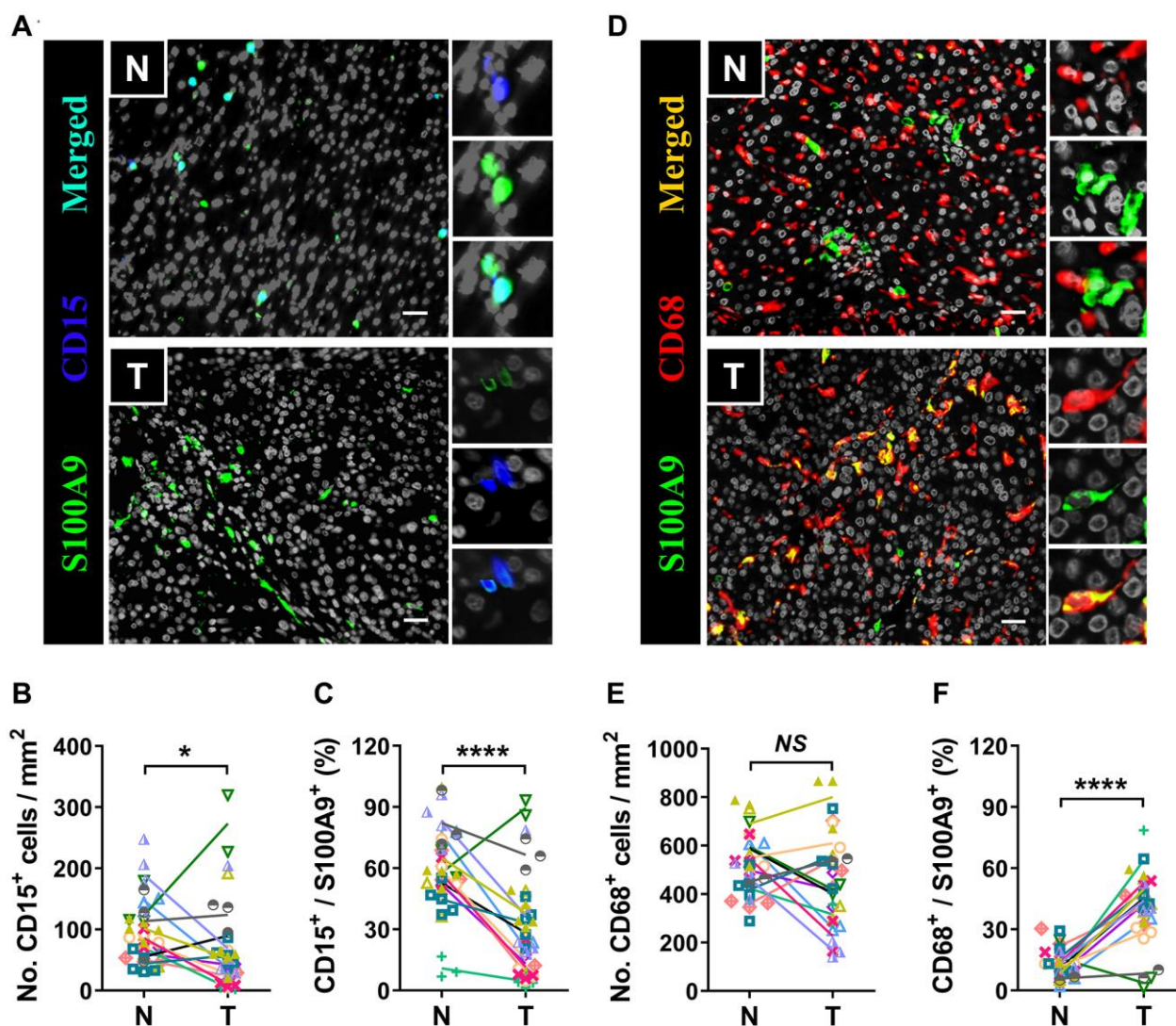


Figure 6. Myeloid cells are the major source of S100A9. Multiple immunofluorescence staining shows DAPI (gray), S100A9 (green), CD15 (blue, A), and CD68 (red, D) expression and coexpression (double-positive cells) in the N and T regions. Quantification of CD15⁺ (B) and CD68⁺ (E) cell densities in the T and N regions ($n = 12$). (C) The percentages of S100A9⁺CD15⁺ cells among the total S100A9⁺ cells in the N and T regions. (F) The percentages of S100A9⁺CD68⁺ cells among the total S100A9⁺ cells in the N and T regions. ($n = 12$). Scale bar = 25 μ m. N, nontumor, T, tumor. * $P < 0.05$, **** $P < 0.0001$, NS, no significance.

prognosis. Furthermore, multivariate analyses revealed that S100A9⁺ cell number was an independent and significant prognostic factor in HCC. Consistent with our results, previous studies showed that S100A9⁺ cell density was associated with a poor prognosis in patients with other cancers, such as clear cell renal cell carcinoma [26], invasive ductal carcinoma of the breast [24], and non-small cell lung cancer [21].

S100A9 plays an important role in malignant development and cancer progression by triggering protumor immune responses. Previous studies have shown that S100A9 acts as a chemotactic molecule to recruit inflammatory cells or immunocytes, such as MDSCs and neutrophils [27, 28], to the tumor microenvironment, resulting in a proinflammatory microenvironment that promotes tumor progression [29, 30]. We found that high S100A9 expression in HCC patients was linked to macrophage chemotaxis, mast cell activation, mononuclear cell migration, and eosinophil migration. These immune cells in the tumor microenvironment can produce vast amounts of cytokines, growth factors and chemokines as well as reactive oxygen species (ROS) and nitric oxide (NO), which stimulate proliferation, promote stemness, prevent apoptosis, induce morphogenesis, mediate DNA damage in epithelial cells [31–33], and promote the survival and migration of cancer cells [34–37]. Furthermore, S100A9 also acts as a novel NF- κ B target gene in HCC cells [36, 38]. S100A9 can efficiently activate immune cells in the microenvironment to secrete TNF- α and maintain the protumor phenotype [39, 40]. Consequently, S100A9 might control tumor progression by acting either directly on tumor cells or indirectly on the tumor microenvironment.

Interestingly, S100A9 staining of the nontumor tissue of HCC patients provided prognostic information. Current evidence has demonstrated that tumor-adjacent, morphologically normal tissue is not completely normal [41–43]. S100A9 was expressed in nontumor tissue, suggesting the early involvement of the proteins in HCC.

However, this study has certain limitations. The underlying molecular mechanisms regulating distinct cell sources of S100A9⁺ cells in nontumoral and tumoral regions are still largely unclear, further studies are needed. Nevertheless, our current study identified that high S100A9 expression was associated with poor OS and a high recurrence risk in patients with HCC. Consequently, S100A9 expression could be considered a significant prognostic marker in patients with HCC.

MATERIALS AND METHODS

Patients and tissue specimens

This study was approved by the Ethics Committee of Sun Yat-sen University Cancer Center (SYSUCC). A total of 382 patients with pathologically confirmed HCC who underwent surgery at the SYSUCC from June 21, 2006 to September 17, 2010 were included in this study. The patients provided informed consent for participation in the present study. The patients did not receive any immunotherapy or neoadjuvant therapy before the operation. The clinical data of the patients were extracted from their electronic medical records and are listed in Table 1.

The clinical stage of tumors was determined according to the tumor-node-metastasis (TNM) classification system of the American Joint Committee on Cancer (AJCC, 2018–01–01, 8th edition). The follow-up period ended in July 2014, and the median survival time was 63 months (range, 1 – 121 months). Recurrence was diagnosed pathologically via surgical biopsy and/or radiologically via computed tomography or positron emission tomography. OS was defined as the length of time between surgery and death or the last follow-up examination.

Analysis of data from The Cancer Genome Atlas (TCGA)

Data on the expression levels of the *S100A9* gene in human HCC were obtained from TCGA up to April 17, 2020. Samples included only those that were annotated as “untreated, primary HCC”. A total of 365 HCC tissues and 50 normal tissues were selected based on the official TCGA-liver hepatocellular carcinoma (LIHC) dataset. *S100A9* gene expression (as transcripts per kilobase million (TPM) values) and corresponding clinical and pathological data of these samples were downloaded and processed as previously described. The gene expression TPM data of *S100A9* are shown in Supplementary Table 1.

Gene ontology (GO) analysis and gene set enrichment analysis (GSEA)

According to the expression level of S100A9 in the tumor tissues of 365 patients in the TCGA-LIHC database, the patients were divided into high and low groups (low, $n = 183$; high, $n = 182$).

Under the condition of $P < 0.05$, a total of 3493 genes were highly expressed in the *S100A9*^{high} group (the fold change of high group/low group > 2), and 399 genes were highly expressed in the *S100A9*^{low} group (the fold

Table 1. Correlation between clinicopathological parameters and the density of S100A9⁺ cells.

Characteristics	No. N-S100A9 ⁺ (%)		<i>P</i> value*	No. T-S100A9 ⁺ (%)		<i>P</i> value*
	Low (No. 191)	High (No. 191)		Low (No. 191)	High (No. 191)	
Sex						
female	30 (7.85)	14 (3.66)	0.010	28 (7.33)	16 (4.19)	0.054
male	161 (42.15)	177 (46.34)		163 (42.67)	175 (45.81)	
Age, years						
≤ 50	97 (25.39)	100 (26.18)	0.759	95 (24.87)	102 (26.70)	0.474
> 50	94 (24.61)	91 (23.82)		96 (25.13)	89 (23.30)	
HBsAg						
negative	23 (6.02)	16 (4.19)	0.237	20 (5.24)	19 (4.97)	0.866
positive	168 (43.98)	175 (45.81)		171 (44.76)	172 (45.03)	
AFP, ng/mL						
≤ 25	77 (20.16)	60 (15.71)	0.070	65 (17.02)	72 (18.85)	0.455
> 25	114 (29.84)	131 (34.29)		126 (32.98)	119 (31.15)	
ALT, U/L						
≤ 40	117 (30.63)	102 (26.70)	0.121	106 (27.75)	113 (29.58)	0.469
> 40	74 (19.37)	89 (23.30)		85 (22.25)	78 (20.42)	
Cirrhosis[†]						
absent	39 (10.43)	42 (11.23)	0.706	45 (12.03)	36 (9.63)	0.236
present	148 (39.57)	145 (38.77)		141 (37.70)	152 (40.64)	
Differentiation[†]						
I + II	154 (40.63)	141 (37.20)	0.131	151 (39.84)	144 (37.99)	0.248
III + IV	36 (9.50)	48 (12.66)		37 (9.76)	47 (12.40)	
Tumor multiplicity						
single	145 (37.96)	135 (35.34)	0.247	146 (38.22)	134 (35.08)	0.165
multiple	46 (12.04)	56 (14.66)		45 (11.78)	57 (14.92)	
Tumor size, cm						
≤ 5	117 (30.63)	71 (18.59)	< 0.001	93 (24.35)	95 (24.87)	0.838
> 5	74 (19.37)	120 (31.41)		98 (25.65)	96 (25.13)	
BCLC						
A	137 (35.86)	108 (28.27)	0.002	130 (34.03)	115 (30.10)	0.110
B + C	54 (14.14)	83 (21.73)		61 (15.97)	76 (19.90)	
TNM stage						
I + II	153 (40.05)	122 (31.94)	< 0.001	142 (37.17)	133 (34.82)	0.305
III + IV	38 (9.95)	69 (18.06)		49 (12.83)	58 (15.18)	

[†]Data were missing in these variables for some patients.

* χ^2 test. Significant *P* values (< 0.05) are shown in bold.

change of high group/low group < 0.5). These differentially expressed genes are shown in Supplementary Table 2. The top 30 GO terms (Supplementary Table 3) of the 3493 genes highly expressed in the S100A9^{high} group were analyzed using

GO enrichment tools (<http://enrich.sbio.com/index/ga.asp>).

All transcriptome expression results of S100A9^{low} and 182 S100A9^{high} patients were subjected to 50 hallmark

gene analyses of sets by using GSEA software (version 4.0.2, <http://software.broadinstitute.org/gsea/index.jsp>). The detailed results are shown in Supplementary Table 4.

Immunohistochemistry (IHC) and immunofluorescence

A tissue microarray (TMA) was constructed, and the slides were incubated with a rabbit monoclonal primary antibody against S100A9 (34425, 1:2000, Cell Signaling Technology, USA) at 4°C overnight. The sections were stained using an Envision system (Dako; Carpinteria, CA, USA) as previously described [44].

Double immunofluorescent staining was performed as previously described [45]. Briefly, formalin-fixed paraffin-embedded (FFPE) sections were incubated at 4°C overnight with the following primary antibodies: mouse anti-human CD15 (1:200; ZSBio, China); CD68 (1:200; Dako Cytomatin, USA); CD3 (1:200; ZSBio, China); rabbit anti-human CD20 (1:200; Abcam, UK); CD34 (1:200; ZSBio, China); and CD56 (NCAM1) (1:1000; Sino Biological Inc, China). The sections were then incubated for 30 min at 37°C with a mixture of primary-antibody matched fluorescently labeled secondary antibodies (1:500; Invitrogen; CA, USA).

Image analysis

Immunohistochemically and fluorescently stained sections were scanned at a magnification of $\times 20$ using the Aperio Digital Pathology Scanner (Leica Biosystems Inc., Germany) to capture a digital whole slide image. Digital image analysis for quantification of the staining for S100A9, CD34, CD56, CD20, CD3, CD15 and CD68 was measured using Aperio ScanScope AT Turbo, eSlide Manager and ImageScope software (V12.3.3.7014; Leica Biosystems, Vista, CA, USA) in accordance with the manufacturer's recommendations. The 3 most representative high-power fields were captured for each tumor and nontumor region in all specimens. All measurements were performed by the same researcher, who was blinded to the histologic and patient survival data, to prevent interoperator variability. Moreover, the protein expression level of S100A9 (cells/mm²) in the immunohistochemical staining of the tissue microarray is shown in Supplementary Table 5.

Statistical analyses

All statistical analyses were performed using SPSS version 25.0 (SPSS Inc., Chicago, IL, USA) and GraphPad Prism (version 8). The Kolmogorov-Smirnov test and Shapiro-Wilk test were used to analyze

normality. The significance of differences between groups was determined by the Mann-Whitney test and Wilcoxon matched-pairs signed-rank test. Pearson's correlation was used to evaluate the correlation between investigator count and computer count, and to evaluate the correlation of variables with immune cell infiltration. Survival curves were assessed by Kaplan-Meier analysis with the log-rank test. The Cox proportional hazards model was used to identify prognostic factors through univariate and multivariate analyses. The statistical significance of differences between groups was determined using the two-tailed Student's *t*-test, where differences with $P < 0.05$ were considered significant.

Ethics approval and consent to participate

All patients' samples were anonymously coded in accordance with local ethical guidelines (as stipulated by the Declaration of Helsinki), and written informed consent was provided. The Review Board of Sun Yat-sen University Cancer Center approved the study protocol.

AUTHOR CONTRIBUTIONS

J.L., J.Z.L., and L.L. designed the experiments. J.L., J.Z.L., J.X. and Y.X. performed the experiments. J.L. and J.Z.L. analyzed the data. L.L. and J.L. wrote the manuscript. W.P.W. and L.Z. supervised the project.

CONFLICTS OF INTEREST

The authors declare no conflicts of interest related to this study.

FUNDING

This work was supported by project grants from the National Natural Science Foundation of China (31900651 to J.L.), the Guangdong Basic and Applied Basic Research Foundation (2021A1515012620 to J.L.), and the Fundamental Research Funds for the Central Universities (20ykpy10 to J.L.).

REFERENCES

1. Siegel RL, Miller KD, Jemal A. Cancer statistics, 2018. *CA Cancer J Clin.* 2018; 68:7–30. <https://doi.org/10.3322/caac.21442> PMID:[29313949](https://pubmed.ncbi.nlm.nih.gov/29313949/)
2. Bray F, Ferlay J, Soerjomataram I, Siegel RL, Torre LA, Jemal A. Global cancer statistics 2018: GLOBOCAN estimates of incidence and mortality worldwide for 36 cancers in 185 countries. *CA Cancer J Clin.* 2018; 68:394–424.

- <https://doi.org/10.3322/caac.21492>
PMID:30207593
3. Prieto J, Melero I, Sangro B. Immunological landscape and immunotherapy of hepatocellular carcinoma. *Nat Rev Gastroenterol Hepatol*. 2015; 12:681–700.
<https://doi.org/10.1038/nrgastro.2015.173>
PMID:26484443
 4. Yang H, Yang Y, Dou J, Cui R, Cheng Z, Han Z, Liu F, Yu X, Zhou X, Yu J, Liang P. Cholecystectomy is associated with higher risk of recurrence after microwave ablation of hepatocellular carcinoma: a propensity score matching analysis. *Cancer Biol Med*. 2020; 17:478–91.
<https://doi.org/10.20892/j.issn.2095-3941.2019.0246>
PMID:32587783
 5. Zhang XF, Yang X, Jia HL, Zhu WW, Lu L, Shi W, Zhang H, Chen JH, Tao YF, Wang ZX, Yang J, Wang LX, Lu M, et al. Bcl-2 expression is a poor predictor for hepatocellular carcinoma prognosis of andropause-age patients. *Cancer Biol Med*. 2016; 13:459–68.
<https://doi.org/10.20892/j.issn.2095-3941.2016.0077>
PMID:28154777
 6. Wang K, Chen X, Jin C, Mo J, Jiang H, Yi B, Chen X. A novel immune-related genes prognosis biomarker for hepatocellular carcinoma. *Aging (Albany NY)*. 2020; 13:675–93.
<https://doi.org/10.18632/aging.202173>
PMID:33260154
 7. Gebhardt C, Németh J, Angel P, Hess J. S100A8 and S100A9 in inflammation and cancer. *Biochem Pharmacol*. 2006; 72:1622–31.
<https://doi.org/10.1016/j.bcp.2006.05.017>
PMID:16846592
 8. Salama I, Malone PS, Mihaimeed F, Jones JL. A review of the S100 proteins in cancer. *Eur J Surg Oncol*. 2008; 34:357–64.
<https://doi.org/10.1016/j.ejso.2007.04.009>
PMID:17566693
 9. Tidehag V, Hammarsten P, Egevad L, Granfors T, Stattin P, Leanderson T, Wikström P, Josefsson A, Hägglöf C, Bergh A. High density of S100A9 positive inflammatory cells in prostate cancer stroma is associated with poor outcome. *Eur J Cancer*. 2014; 50:1829–35.
<https://doi.org/10.1016/j.ejca.2014.03.278>
PMID:24726733
 10. Zhou M, Li M, Liang X, Zhang Y, Huang H, Feng Y, Wang G, Liu T, Chen Z, Pei H, Chen Y. The Significance of Serum S100A9 and TNC Levels as Biomarkers in Colorectal Cancer. *J Cancer*. 2019; 10:5315–23.
<https://doi.org/10.7150/jca.31267>
PMID:31632476
 11. Nedjadi T, Evans A, Sheikh A, Barerra L, Al-Ghamdi S, Oldfield L, Greenhalf W, Neoptolemos JP, Costello E. S100A8 and S100A9 proteins form part of a paracrine feedback loop between pancreatic cancer cells and monocytes. *BMC Cancer*. 2018; 18:1255.
<https://doi.org/10.1186/s12885-018-5161-4>
PMID:30558665
 12. Zhao Z, Zhang C, Zhao Q. S100A9 as a novel diagnostic and prognostic biomarker in human gastric cancer. *Scand J Gastroenterol*. 2020; 55:338–46.
<https://doi.org/10.1080/00365521.2020.1737883>
PMID:32172630
 13. Meng J, Gu F, Fang H, Qu B. Elevated Serum S100A9 Indicated Poor Prognosis in Hepatocellular Carcinoma after Curative Resection. *J Cancer*. 2019; 10:408–15.
<https://doi.org/10.7150/jca.28409>
PMID:30719134
 14. Huang CH, Kuo CJ, Liang SS, Chi SW, Hsi E, Chen CC, Lee KT, Chiou SH. Onco-proteogenomics identifies urinary S100A9 and GRN as potential combinatorial biomarkers for early diagnosis of hepatocellular carcinoma. *BBA Clin*. 2015; 3:205–13.
<https://doi.org/10.1016/j.bbaci.2015.02.004>
PMID:26675302
 15. Choi JH, Shin NR, Moon HJ, Kwon CH, Kim GH, Song GA, Jeon TY, Kim DH, Kim DH, Park DY. Identification of S100A8 and S100A9 as negative regulators for lymph node metastasis of gastric adenocarcinoma. *Histol Histopathol*. 2012; 27:1439–48.
<https://doi.org/10.14670/HH-27.1439>
PMID:23018243
 16. Fan B, Zhang LH, Jia YN, Zhong XY, Liu YQ, Cheng XJ, Wang XH, Xing XF, Hu Y, Li YA, Du H, Zhao W, Niu ZJ, et al. Presence of S100A9-positive inflammatory cells in cancer tissues correlates with an early stage cancer and a better prognosis in patients with gastric cancer. *BMC Cancer*. 2012; 12:316.
<https://doi.org/10.1186/1471-2407-12-316>
PMID:22838504
 17. Feng PH, Lee KY, Chang YL, Chan YF, Kuo LW, Lin TY, Chung FT, Kuo CS, Yu CT, Lin SM, Wang CH, Chou CL, Huang CD, Kuo HP. CD14(+)S100A9(+) monocytic myeloid-derived suppressor cells and their clinical relevance in non-small cell lung cancer. *Am J Respir Crit Care Med*. 2012; 186:1025–36.
<https://doi.org/10.1164/rccm.201204-0636OC>
PMID:22955317
 18. Newman AM, Liu CL, Green MR, Gentles AJ, Feng W, Xu Y, Hoang CD, Diehn M, Alizadeh AA. Robust enumeration of cell subsets from tissue expression profiles. *Nat Methods*. 2015; 12:453–57.
<https://doi.org/10.1038/nmeth.3337>
PMID:25822800

19. Donato R, Cannon BR, Sorci G, Riuzzi F, Hsu K, Weber DJ, Geczy CL. Functions of S100 proteins. *Curr Mol Med*. 2013; 13:24–57.
<https://doi.org/10.2174/156652413804486214>
PMID:[22834835](https://pubmed.ncbi.nlm.nih.gov/22834835/)
20. Goyette J, Geczy CL. Inflammation-associated S100 proteins: new mechanisms that regulate function. *Amino Acids*. 2011; 41:821–42.
<https://doi.org/10.1007/s00726-010-0528-0>
PMID:[20213444](https://pubmed.ncbi.nlm.nih.gov/20213444/)
21. Kawai H, Minamiya Y, Takahashi N. Prognostic impact of S100A9 overexpression in non-small cell lung cancer. *Tumour Biol*. 2011; 32:641–46.
<https://doi.org/10.1007/s13277-011-0163-8>
PMID:[21369941](https://pubmed.ncbi.nlm.nih.gov/21369941/)
22. Hermani A, Hess J, De Servi B, Medunjanin S, Grobholz R, Trojan L, Angel P, Mayer D. Calcium-binding proteins S100A8 and S100A9 as novel diagnostic markers in human prostate cancer. *Clin Cancer Res*. 2005; 11:5146–52.
<https://doi.org/10.1158/1078-0432.CCR-05-0352>
PMID:[16033829](https://pubmed.ncbi.nlm.nih.gov/16033829/)
23. Yan LL, Huang YJ, Yi X, Yan XM, Cai Y, He Q, Han ZJ. Effects of silencing S100A8 and S100A9 with small interfering RNA on the migration of CNE1 nasopharyngeal carcinoma cells. *Oncol Lett*. 2015; 9:2534–40.
<https://doi.org/10.3892/ol.2015.3090>
PMID:[26137102](https://pubmed.ncbi.nlm.nih.gov/26137102/)
24. Arai K, Takano S, Teratani T, Ito Y, Yamada T, Nozawa R. S100A8 and S100A9 overexpression is associated with poor pathological parameters in invasive ductal carcinoma of the breast. *Curr Cancer Drug Targets*. 2008; 8:243–52.
<https://doi.org/10.2174/156800908784533445>
PMID:[18537548](https://pubmed.ncbi.nlm.nih.gov/18537548/)
25. Arai K, Yamada T, Nozawa R. Immunohistochemical investigation of migration inhibitory factor-related protein (MRP)-14 expression in hepatocellular carcinoma. *Med Oncol*. 2000; 17:183–88.
<https://doi.org/10.1007/BF02780526>
PMID:[10962528](https://pubmed.ncbi.nlm.nih.gov/10962528/)
26. Koh HM, An HJ, Ko GH, Lee JH, Lee JS, Kim DC, Song DH. Prognostic role of S100A9 expression in patients with clear cell renal cell carcinoma. *Medicine (Baltimore)*. 2019; 98:e17188.
<https://doi.org/10.1097/MD.00000000000017188>
PMID:[31577709](https://pubmed.ncbi.nlm.nih.gov/31577709/)
27. Ryckman C, Vandal K, Rouleau P, Talbot M, Tessier PA. Proinflammatory activities of S100: proteins S100A8, S100A9, and S100A8/A9 induce neutrophil chemotaxis and adhesion. *J Immunol*. 2003; 170:3233–42.
<https://doi.org/10.4049/jimmunol.170.6.3233>
PMID:[12626582](https://pubmed.ncbi.nlm.nih.gov/12626582/)
28. Seizer P, Schönberger T, Schött M, Lang MR, Langer HF, Bigalke B, Krämer BF, Borst O, Daub K, Heidenreich O, Schmidt R, Lindemann S, Herouy Y, et al. EMMPRIN and its ligand cyclophilin A regulate MT1-MMP, MMP-9 and M-CSF during foam cell formation. *Atherosclerosis*. 2010; 209:51–57.
<https://doi.org/10.1016/j.atherosclerosis.2009.08.029>
PMID:[19758589](https://pubmed.ncbi.nlm.nih.gov/19758589/)
29. Alkhateeb T, Kumbhare A, Bah I, Youssef D, Yao ZQ, McCall CE, El Gazzar M. S100A9 maintains myeloid-derived suppressor cells in chronic sepsis by inducing miR-21 and miR-181b. *Mol Immunol*. 2019; 112:72–81.
<https://doi.org/10.1016/j.molimm.2019.04.019>
PMID:[31078118](https://pubmed.ncbi.nlm.nih.gov/31078118/)
30. Alexaki VI, May AE, Fujii C, von Ungern-Sternberg SNI, Mund C, Gawaz M, Chavakis T, Seizer P. S100A9 induces monocyte/ macrophage migration via EMMPRIN. *Thromb Haemost*. 2017; 117:636–39.
<https://doi.org/10.1160/TH16-06-0434>
PMID:[27808344](https://pubmed.ncbi.nlm.nih.gov/27808344/)
31. Wang Y, Yin K, Tian J, Xia X, Ma J, Tang X, Xu H, Wang S. Granulocytic Myeloid-Derived Suppressor Cells Promote the Stemness of Colorectal Cancer Cells through Exosomal S100A9. *Adv Sci (Weinh)*. 2019; 6:1901278.
<https://doi.org/10.1002/advs.201901278>
PMID:[31559140](https://pubmed.ncbi.nlm.nih.gov/31559140/)
32. Laouedj M, Tardif MR, Gil L, Raquil MA, Lachhab A, Pelletier M, Tessier PA, Barabé F. S100A9 induces differentiation of acute myeloid leukemia cells through TLR4. *Blood*. 2017; 129:1980–90.
<https://doi.org/10.1182/blood-2016-09-738005>
PMID:[28137827](https://pubmed.ncbi.nlm.nih.gov/28137827/)
33. De Ponti A, Wiechert L, Schneller D, Pusterla T, Langerich T, Hogg N, Vogel A, Schirmacher P, Hess J, Angel P. A pro-tumorigenic function of S100A8/A9 in carcinogen-induced hepatocellular carcinoma. *Cancer Lett*. 2015; 369:396–404.
<https://doi.org/10.1016/j.canlet.2015.09.005>
PMID:[26404752](https://pubmed.ncbi.nlm.nih.gov/26404752/)
34. Wu R, Duan L, Cui F, Cao J, Xiang Y, Tang Y, Zhou L. S100A9 promotes human hepatocellular carcinoma cell growth and invasion through RAGE-mediated ERK1/2 and p38 MAPK pathways. *Exp Cell Res*. 2015; 334:228–38.
<https://doi.org/10.1016/j.yexcr.2015.04.008>
PMID:[25907296](https://pubmed.ncbi.nlm.nih.gov/25907296/)
35. Lv Z, Li W, Wei X. S100A9 promotes prostate cancer cell invasion by activating TLR4/NF-κB/integrin

- β 1/FAK signaling. *Onco Targets Ther.* 2020; 13:6443–52.
<https://doi.org/10.2147/OTT.S192250>
PMID:[32884282](https://pubmed.ncbi.nlm.nih.gov/32884282/)
36. Duan L, Wu R, Zhang X, Wang D, You Y, Zhang Y, Zhou L, Chen W. HBx-induced S100A9 in NF- κ B dependent manner promotes growth and metastasis of hepatocellular carcinoma cells. *Cell Death Dis.* 2018; 9:629.
<https://doi.org/10.1038/s41419-018-0512-2>
PMID:[29795379](https://pubmed.ncbi.nlm.nih.gov/29795379/)
37. Hibino T, Sakaguchi M, Miyamoto S, Yamamoto M, Motoyama A, Hosoi J, Shimokata T, Ito T, Tsuboi R, Huh NH. S100A9 is a novel ligand of EMMPRIN that promotes melanoma metastasis. *Cancer Res.* 2013; 73:172–83.
<https://doi.org/10.1158/0008-5472.CAN-11-3843>
PMID:[23135911](https://pubmed.ncbi.nlm.nih.gov/23135911/)
38. Németh J, Stein I, Haag D, Riehl A, Longerich T, Horwitz E, Breuhahn K, Gebhardt C, Schirmacher P, Hahn M, Ben-Neriah Y, Pikarsky E, Angel P, Hess J. S100A8 and S100A9 are novel nuclear factor κ B target genes during malignant progression of murine and human liver carcinogenesis. *Hepatology.* 2009; 50:1251–62.
<https://doi.org/10.1002/hep.23099>
PMID:[19670424](https://pubmed.ncbi.nlm.nih.gov/19670424/)
39. Simard JC, Cesaro A, Chapeton-Montes J, Tardif M, Antoine F, Girard D, Tessier PA. S100A8 and S100A9 induce cytokine expression and regulate the NLRP3 inflammasome via ROS-dependent activation of NF- κ B(1.). *PLoS One.* 2013; 8:e72138.
<https://doi.org/10.1371/journal.pone.0072138>
PMID:[23977231](https://pubmed.ncbi.nlm.nih.gov/23977231/)
40. Chen B, Miller AL, Rebelatto M, Brewah Y, Rowe DC, Clarke L, Czapiga M, Rosenthal K, Imamichi T, Chen Y, Chang CS, Chowdhury PS, Naiman B, et al. S100A9 induced inflammatory responses are mediated by distinct damage associated molecular patterns (DAMP) receptors *in vitro* and *in vivo*. *PLoS One.* 2015; 10:e0115828.
<https://doi.org/10.1371/journal.pone.0115828>
PMID:[25706559](https://pubmed.ncbi.nlm.nih.gov/25706559/)
41. Halin S, Hammarsten P, Adamo H, Wikström P, Bergh A. Tumor indicating normal tissue could be a new source of diagnostic and prognostic markers for prostate cancer. *Expert Opin Med Diagn.* 2011; 5:37–47.
<https://doi.org/10.1517/17530059.2011.540009>
PMID:[23484475](https://pubmed.ncbi.nlm.nih.gov/23484475/)
42. Halin S, Rudolfsson SH, Van Rooijen N, Bergh A. Extratumoral macrophages promote tumor and vascular growth in an orthotopic rat prostate tumor model. *Neoplasia.* 2009; 11:177–86.
<https://doi.org/10.1593/neo.81338>
PMID:[19177202](https://pubmed.ncbi.nlm.nih.gov/19177202/)
43. Hägglöf C, Bergh A. The stroma—a key regulator in prostate function and malignancy. *Cancers (Basel).* 2012; 4:531–48.
<https://doi.org/10.3390/cancers4020531>
PMID:[24213323](https://pubmed.ncbi.nlm.nih.gov/24213323/)
44. Liao J, Zeng DN, Li JZ, Hua QM, Xiao Z, He C, Mao K, Zhu LY, Chu Y, Wen WP, Zheng L, Wu Y. Targeting adenosinergic pathway enhances the anti-tumor efficacy of sorafenib in hepatocellular carcinoma. *Hepatol Int.* 2020; 14:80–95.
<https://doi.org/10.1007/s12072-019-10003-2>
PMID:[31802389](https://pubmed.ncbi.nlm.nih.gov/31802389/)
45. Chu Y, Liao J, Li J, Wang Y, Yu X, Wang J, Xu X, Xu L, Zheng L, Xu J, Li L. CD103⁺ tumor-infiltrating lymphocytes predict favorable prognosis in patients with esophageal squamous cell carcinoma. *J Cancer.* 2019; 10:5234–43.
<https://doi.org/10.7150/jca.30354>
PMID:[31602274](https://pubmed.ncbi.nlm.nih.gov/31602274/)

SUPPLEMENTARY MATERIALS

Supplementary Tables

Please browse Full Text version to see the data of Supplementary Tables 1 to 5.

Supplementary Table 1. TCGA Database for S100A9 Expression.

Supplementary Table 2. IHC Detection for S100A9 Expression.

Supplementary Table 3. Differentially Expressed Genes for S100A9_high vs S100A9_low Group.

Supplementary Table 4. Top 30 of GO Enrichment.

Supplementary Table 5. GSEA Analysis for Hallmark Gene Sets.